Abstract

The mechanical properties of bio adhesives in oral care application are expected to be critical in defining the stability and release of devices such as dentures from the oral tissue. A multiscale experimental mechanical approach is used to evaluate the performance of denture adhesive materials. The inherent mechanical behaviour of denture fixatives was examined by separating adhesive material from a representative polymethyl methacrylate (PMMA) surface using atomic force microscopy (AFM) approaches and compared to macroscopic mechanical testing. Failure of denture adhesive material was found to be critically dependent on the formation of fibrillar structures within the adhesive. Small scale mechanical testing provides evidence for the mechanical properties of the fibrillar structures formed within the adhesive in macroscopic mechanical testing and indicates the importance of the forces required to fail the adhesive at these small length scales in controlling both the maximum forces sustained by the bulk material as well as the ease of separating the adhesive from PMMA surfaces. Our results are important in defining the performance of denture fixative materials and their control of adhesive behaviour, allowing the potential to tune properties required in the adhesion and removal of dentures.

1. Introduction

Complex processes regulate the adhesion of biomaterials to tissues and other interfaces [1-5], with the magnitude of such interactions defining the overall performance of implants. In particular, understanding the mechanical properties of the adhesive at the interface with the device and tissue are required for evaluation of resultant adhesive performance [5-7]. Adhesives for dentures are particularly demanding and need to provide fixation of the denture within the aggressive environment of the oral cavity but allow relatively effective removal on demand [8-13]. The adhesion of dentures is almost contradictory as both high adhesion for fixing and low adhesion for easy of removal are required. The potential sensitivity of adhesion in controlling denture fixing and removal motivates the need for techniques that are able to comprehensively evaluate the adhesion process. The relationship between molecular interactions at interfaces and in the bulk of the adhesive involves evaluation of stress transfer and failure mechanisms that are currently poorly defined. Methods that quantify structure-property relationships controlling the behaviour of such interfaces are important in understanding and designing implants and adhesives in the biomedical field, including for oral care applications. From fundamental considerations, electrostatic interactions and hydrogen bonding are known to significantly contribute to the bulk mechanical and rheological properties of biomaterials used for dental adhesive applications [14]. However, the role of these

interactions, together with other hydrophobic interactions occurring at the surface of implants and denture, on the failure of adhesive remains unclear. Chemical design of biomaterials is therefore important in controlling the failure of the adhesive, specifically at interfaces or within the bulk, and enables tailoring of the mechanical properties of the adhesive to function. The location of failure occurs either at an interface (adhesive failure) or in the bulk of the adhesive (cohesive failure) has been shown to be particularly important in defining resultant adhesive performance [15, 16]. Suitable experimental techniques are required to both measure the mechanical properties of the dental adhesive directly and relate to the chemistry of the adhesive. Microscale mechanical testing using atomic force microscopy (AFM) is often employed to understand these mechanical properties directly and, as the size considered is relatively small, geometric considerations that dominate at larger lengths can be ignored so that the inherent material chemistry are probed [17-21]. Extension of small-scale mechanical testing has incorporated *in situ* imaging using scanning electron microscopy (SEM) that allows correlation between the mechanical response of a biomaterial and the observed deformation or failure event, the latter being important in defining either adhesive or cohesive failure [17-20]. The powerful combination of small-scale mechanical testing and *in situ* imaging is therefore applicable to denture adhesives to provide quantitative evidence of the influence of chemistry on failure mechanisms. In this work, the mechanical properties of a dental adhesive in contact with poly(methyl methacrylate) (PMMA) dentures was examined. Our approaches aim to correlate the larger macroscopic length scale to more

fundamental microscale behaviour for comprehensive structure-property relationships.

2. Materials and methods

2.1. Overview

Commercially available dental adhesives (GSK, UK), Poligrip®, Ultra Wernets®, Denture Fixative Powder (PDFP) and Poligrip®, Ooze-Control Tip® Denture Adhesive Cream (PDAC), were used in this study. PDFP is composed of poly(methylvinylether/maleic acid) sodium-calcium mixed partial salt, cellulose gum and aroma while PDAC is composed of poly(methylvinylether/maleic acid) sodium-magnesium-zinc mixed partial salt, petrolatum, cellulose gum, mineral oil, silica, poly(methylvinylether/maleic acid), flavour, Red 30 aluminum lake and Red 7 calcium lake. PDAC contains more hydrophobic compounds such as hydrocarbon vehicles (mineral oil and petrolautum), in addition to MVE/MA copolymer. These may affect the hydration of the polymers and gel formation resulting in different adhesion behaviour. Both materials were applied as adhesives to investigate their adhesion behaviour with a PMMA substrate representing a standard denture material. Both PDFP and PDAC were wet by mixing with distilled water at the ratio of 1:1 in a petri dish before mechanical testing. This approach was considered to represent the hydration state of the adhesives in typical usage conditions in the oral cavity for fixing dentures [22]. Adhesion behaviour of PDFP and PDAC with PMMA was investigated

at both the macroscale and microscale to fully characterize their adhesion mechanics, as shown schematically in Fig. 1.
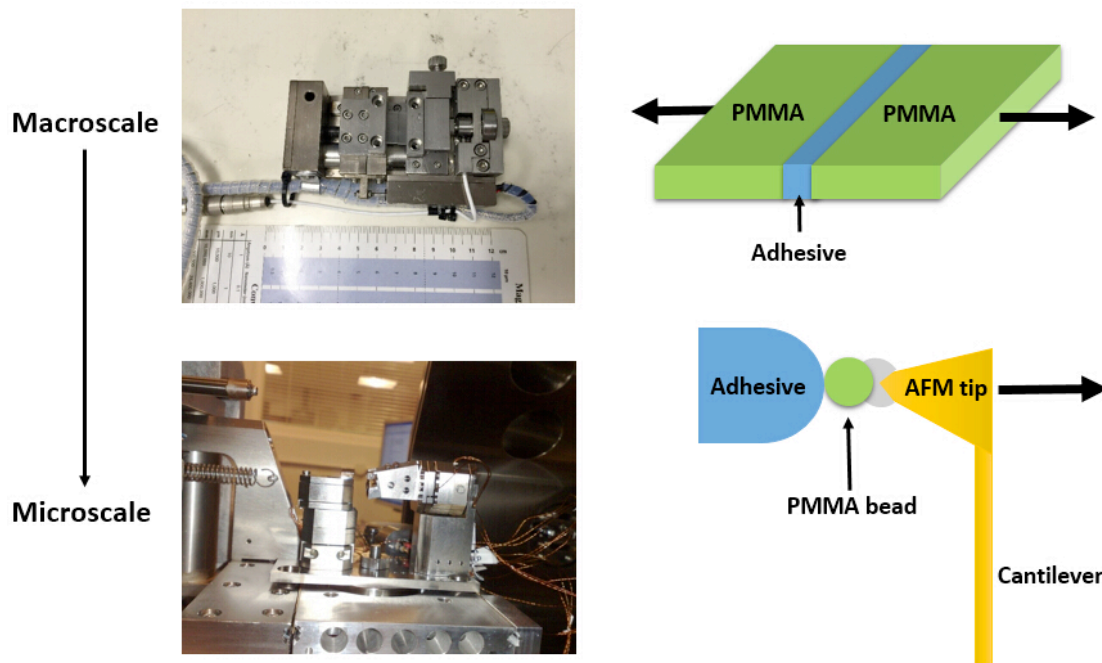
Fig. 1 - Schematic showing the macroscale and microscale tests performed to evaluate the performance of PDFP/PDAC adhesives using (top) a commercial microtester and (bottom) an AFM setup.

2.2. Macroscopic testing

Macroscopic testing was performed by detaching two adhesive-bonded PMMA plates and examining their adhesion properties. Commercial PMMA plates were cut using a circular saw (Struers, Germany) into dimensions of $3 \times 6 \times 15$ mm with the cross section area of 3×6 mm for adhesive attachment. Two PMMA plates were bonded with a small amount (weighted approximately 0.15 ± 0.5 g) of wet adhesive sufficient to fully cover the cross section area and held together by hand for 1 minute before

mounting the two adhesive-bonded PMMA plates on a commercial microtester (Deben, 200 N tensile stage, U.K., as shown in Fig. 1. The microtester was mounted onto a scanning electron microscope (SEM) sample stage within the SEM chamber (Quanta 3D FEG, FEI, EU/USA) so that mechanical testing was observed using the SEM. The opposite ends of each PMMA plate were clamped tightly by the sample grip of the microtester, leaving the two adhesive-bonded cross section surfaces in the middle of the gauge. Initial distance between the two sample grips was calibrated to 10.09 mm. Uniaxial tensile test was performed by translating one of the grips away from the other at a constant rate of 0.5 mm·min^{-1}, causing the two adhesive-bonded cross section surfaces to detach. The force and extension applied to the sample was recorded using the microtester while SEM allowed physical deformation to be related to the mechanical information.

2.3. Nanoscale AFM testing

2.3.1. Sample preparation

Adhesion behaviour between PDFP/PDAC and PMMA was further investigated at smaller length scales to evaluate the relationship between mechanical properties and interfacial chemistry in a geometrically simple setup. Spherical microscale PMMA-coated silica beads were used to study the PDFP/PDAC-PMMA adhesion at the microscale. These microscale experiments were important and allowed comparison with macroscopic testing that incorporates chemistry as well as potentially larger

structural features, such as voids, that may dominate adhesion behaviour. The microbeads were prepared by coating commercial 3.43 μm diameter silica beads (Bangs Laboratories Inc., USA) with PMMA polymer brushes using protocols adapted from the literature [23, 24]. 1 ml of toluene kept under nitrogen was added to 50 mg silica beads and sonicated for 10 minutes until the suspension was cloudy. The bead suspension was then centrifuged at 5000 rpm for 30 s and the toluene allowed to aspire. The sonication and centrifugation process was repeated three times and the beads were finally dispersed in 1 ml toluene. The grafting of the initiator silane monolayer for atom transfer radical polymerisation was carried by adding 50 μl of Et$_3$N and 10 μl silane initiator to the 1 ml silica dispersion followed by shaking overnight. The silica beads with silane initiator were then washed with 1 ml DMF three times, stored in 1 ml DMF and transferred to a refrigerator held at 4°C until polymerisation.

1 ml DMF and 0.5 ml deionized water was added into the 1 ml silica beads dispersion in the reaction vessel, and then degased for 30 minutes with argon bubbling. The monomer solution of bipyridine (167 mg), Cu(II)Br (97 mg), MMA (4.5 ml), deionized water (2 ml), DMF (8 ml) was degased via argon bubbling for 30 minutes while stirring, then Cu(I)Br (62 mg) was quickly added into the solution, followed by another 30 minutes bubbling. A further 2.5 ml of monomer solution was added to the reaction vessels containing 2.5 ml of the particle suspension. Polymerisation was allowed to proceed for 2 hours under argon at room temperature. To terminate the

polymerisation, the reaction mixture was bubbled with compressed air until a blue colouration was observed. The obtained SiO_2-PMMA suspension was centrifuged and washed three times with deionized water and DMF (v/v=1:4) to remove the catalyst and suspended PMMA polymer, during which, sonication was applied to reduce the aggregation. Finally the PMMA-coated beads were dispersed in 1 ml deionized water and stored in a refrigerator before usage. The diameter of the PMMA-coated bead was ~3.53 μm, highlighting an increased silica bead diameter due to the coating, as measure using SEM.

2.3.2. AFM mechanical testing

A small volume of PMMA-coated bead solution was deposited onto a silicon wafer and left overnight to allow solvent evaporation prior to mechanical testing. This step provided a sparse distribution of beads over the silicon wafer surface. A custom built AFM (Attocube GmbH, Germany) integrated within an SEM (Quanta 3D FEG, FEI, EU/USA), as described in previous work [19], was used to attach individual beads to the apex of an AFM tip. The combination of SEM and AFM is effective as the AFM provides high-resolution force information while the SEM gives imaging capabilities. A schematic of the combined AFM–SEM set-up is shown in Fig. 1 and highlights the experimental setup where the AFM tip contacts an individual bead on the silicon wafer surface. Pickup of an individual PMMA-coated bead to the apex of the AFM tip was achieved by first translating the apex of the AFM tip into a droplet of glue (SEMGLU, Kleindiek Nanotechnik GmbH, Germany). Removal of the AFM tip from

the glue caused deposition of a small amount of glue at the apex of the AFM tip. The AFM tip was subsequently moved towards the PMMA-coated beads on the silicon wafer. The beads were confirmed as being dispersed over the silicon wafer surface as shown in Fig. 2a. The AFM tip was translated into contact with an individual bead so that the bead was fixed to the glue at the AFM tip apex as shown in Fig. 2b. The high-vacuum compatible adhesive glue hardens under electron beam irradiation. Relatively low imaging electron currents of 93 pA at 10 kV were used so that the glue remains uncured and deformable. Focusing a high current electron beam of 1.5 nA for approximately 10 minutes on a small area of the glue causes initiation of glue polymerization and subsequent solidification. In this way, the glue solidifies and attaches the bead firmly to the apex of the AFM tip. Fig. 2c shows a SEM micrograph of an individual PMMA-coated bead attached to the apex of the AFM tip.
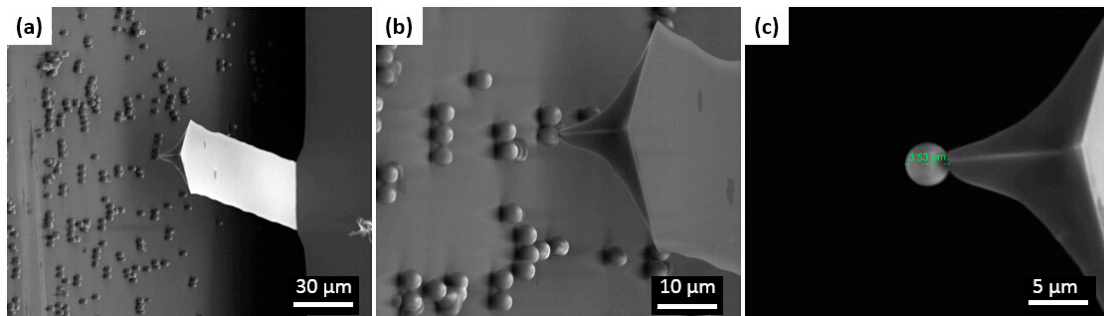
Fig. 2 - (a) SEM micrographs showing (a) the PMMA-coated beads dispersed on the silicon wafer, (b) contact of the AFM tip to one PMMA-coated bead and (c) an individual PMMA-coated bead attached to the apex of the AFM tip. The dimension of the bead was confirmed as 3.53 μm.

The PMMA-coated bead attached to the AFM tip was retained in the AFM setup and wet PDFP and PDAC samples were mounted to the AFM sample stage for adhesion testing. Each adhesive was translated by the piezo positioners of the AFM system until contact with an individual PMMA-coated bead at the apex of the AFM tip and the PDFP or PDAC adhesive surface was achieved. After contact, the AFM tip was retracted away from the sample at a constant rate of 0.2 $\mu m \cdot s^{-1}$ so that interfacial failure and complete separation of the bead from the adhesive occurred. A soft AFM cantilever with a spring constant of 0.13 $N \cdot m^{-1}$, measured using the Sader calibration method [25], was used in this work to provide sufficient force resolution.

2.4. Compositional study using EDS

X-ray energy dispersive spectroscopy (EDS) microanalysis within an SEM (Inspect SEM, FEI Company, EU/USA) was used to investigate the chemical composition of the PMMA cross-sectional surface after failure of the adhesive performed using the Deben microtester. The EDS detection was performed under 10 keV at the working distance of 10 mm. The depth of the layer under analysis with EDS is dependent on the sample and the beam energy of the electron beam, calculated as 5.5 μm using Monte Carlo simulation (Casino v2.42, Can.). Chemical analysis allows understanding of the failure mechanism at the adhesive surface as many adhesives, including those used in this study, contain inorganic ions or fillers. Thus, analysis of a PMMA surface after failure can reveal if inorganics are present, suggesting failure

occurred within the adhesive so that a thin adhesive layer is present at the PMMA surface, or a clean PMMA surface indicating PMMA-adhesive interfacial failure.

3. Results and discussion

3.1. Macroscopic testing

3.1.1. PDFP

Fig. 3 shows a typical force-extension curve of the adhesive recorded during the macroscopic test using PDFP as the adhesive between the two PMMA plates. The plot shows an initial steep slope until a maximum force of ~1.34 N at an extension of ~4 μm was reached, followed by a long yielding phase, associated with fast stress relaxation and high ultimate strains to the maximum adhesive extension of ~371 μm. The yield point A shown in Fig. 3 is a critical transition point between two regions and was correlated with the adhesive behaviour observed using SEM.
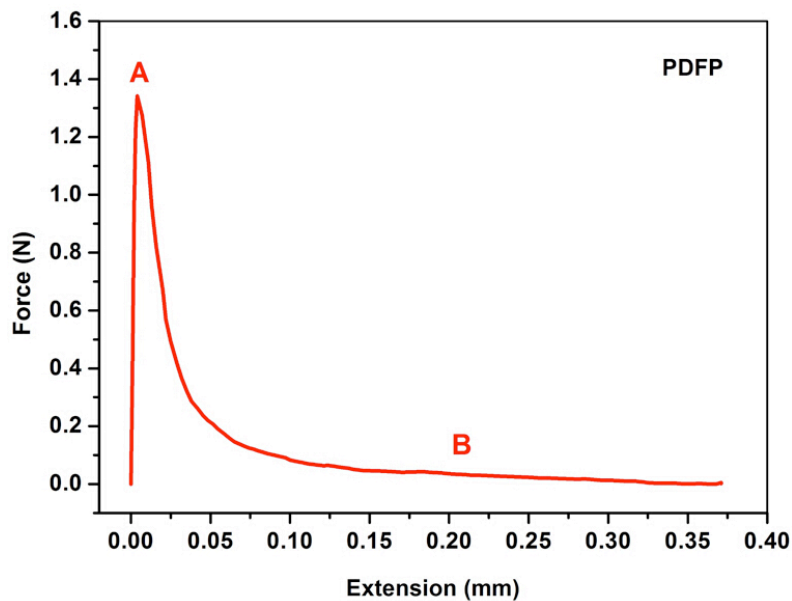
Fig. 3 - Typical force-extension curve recorded during the separation of two PMMA plates adhered together by PDFP.

SEM micrographs of the PDFP adhesive at yielding (point A) are shown in Fig. 4. An adhesive interface between the two PMMA plates was observed in Fig. 4 due to clean PMMA surfaces devoid of polymeric reside, which is indicative adhesive delamination and is proposed to occur at the yielding point. The formation of fibrils in the adhesive clearly shown in Fig. 4d is also observed at this yielding stage.
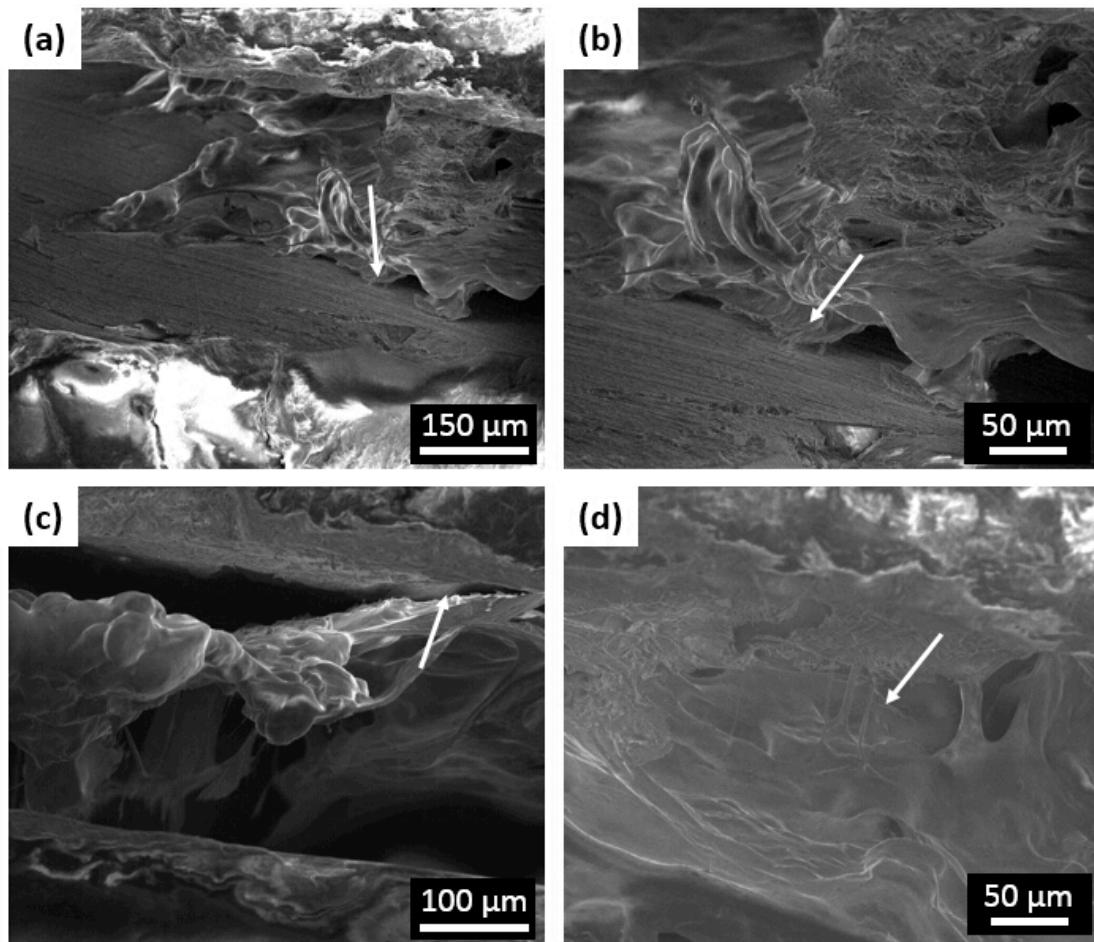
Fig. 4 - Scanning electron micrographs of the PDFP-bonded interface at the yielding point. The images are obtained from different samples and show the delamination behaviour of the PDFP adhesive, indicated by white arrows.

The adhesion behaviour of the PDFP adhesive during force relaxation at higher displacements, as indicated at point B in Fig. 3, was examined using SEM imaging. Fig. 5 indicates further necking of the adhesive fibrils that formed at the yielding point A associated with a reduced contact area between the PMMA plates.
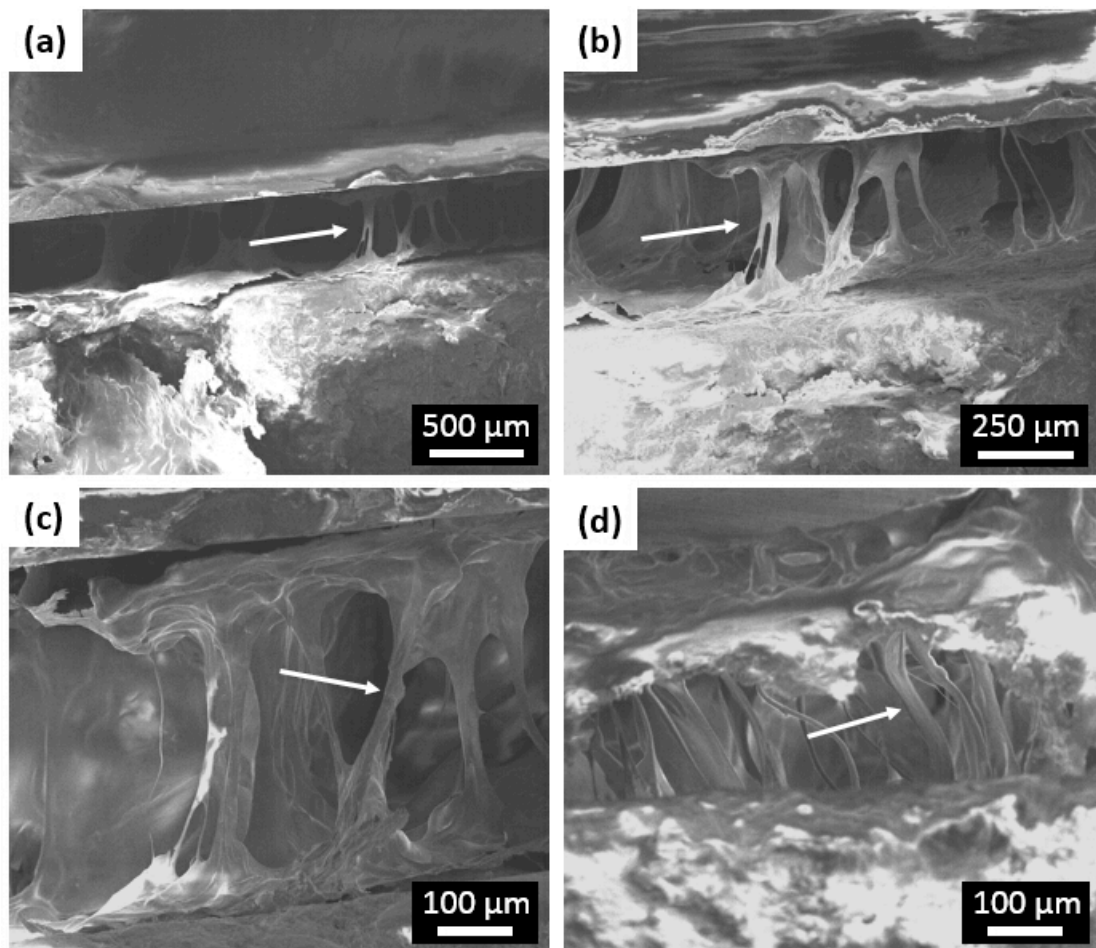
Fig. 5 - Scanning electron micrographs of the PDFP-bonded interfacial failure at higher sample strains. The images are obtained show the deformation behaviour of the

PDFP adhesive at higher strains at a range of magnifications and associated formation of fibrils (indicated by white arrows).

Detachment of the adhesive from the PMMA surface or failure within the adhesive is critical in understanding the adhesive performance and requires chemical evaluation of the evolved surfaces. EDS of sample provided chemical composition of the failed PMMA-adhesive interface. Fig. 6 shows scanning electron micrographs of two PDFP-bound samples taken to failure. Areas A and B in Fig. 6 correspond to extensions A (yielding point) and B (higher strain) in Fig. 3, respectively. These two different areas were imaged with EDS with 5 detecting points on each sample. Table 1 states the measured chemical composition of the interface of both samples. These EDS results indicate the presence of areas displaying a clean PMMA plate surface, highlighted by an absence in Na and areas still coated with the adhesive. Indeed, EDS only shows carbon and oxygen elements for clean PMMA areas, whereas additional Na is detected (as the counter ion of the polyanionic adhesive component of PDFP) in other areas, indicating the presence of adhesive PDFP. This behaviour was not altered as the tensile test proceeded, suggesting that isolated islands of residual adhesive are left at the surface of PMMA after failure. This data confirms that PDFP failure occurs at the interface with the PMMA, leaving areas of the PMMA surface uncovered by the adhesive.
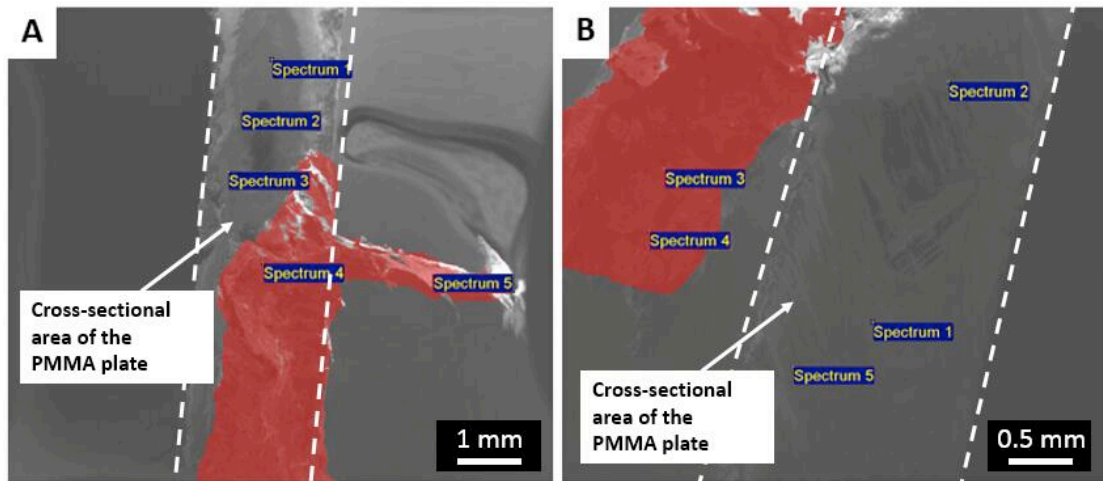
Fig. 6 - SEM images of the cross-sectional area of the PMMA plate with the failed interface of adhesives stretched to extensions A and B in Fig. 5. For both samples, EDS measurements were performed at 5 different locations to probe the chemical composition of the structures imaged, with the red areas indicating the region covered with PDFP adhesive.

Table 1 - Chemical composition (measured by EDS) of different areas for samples taken to extensions corresponding to points A and B in Fig. 3.

Area A	C	O	Na
1	69.93%	30.07%	0
2	70.95%	29.05%	0
3	80.81%	19.19%	0
4	51.15%	44.48%	4.37%
5	53.39%	41.33%	5.29%
Area B	C	O	Na
1	77.45%	22.55%	0
2	71.76%	28.24%	0
3	53.55%	43.13%	3.33%
4	47.62%	44.69%	7.69%
5	79.02%	20.31%	0.67%

Hence, failure of PMMA surfaces bonded by PDFP is proposed as a partial delamination of adhesive from the PMMA surface, followed by necking of the adhesive itself at larger strains. In this second high strain region, local failure of the formed fibrils is expected to be associated with high strain induced polymer chain alignment around defects such as bubbles, as is commonly observed in glassy polymers and are inherent to relatively inhomogeneous [26].

3.1.2. PDAC

The adhesive behaviour of PDAC to PMMA surfaces was studied using the same macroscopic and microscale mechanical testing employed for PDFP. The nature of the PDAC cream, which displays a heterogeneous morphology with mixtures of hydrophilic and hydrophobic domains, is expected to alter bonding to the PMMA surface and subsequent failure mechanism. Specifically, the apolar groups of the PMMA are expected to interact, although weakly, with the hydrophobic domains of the PDAC. PMMA plates were bonded with a small amount of adhesive sufficient to cover the cross section area and held together for 1 min. before mounting the sample on the microtensile tester. The loading rate was kept constant at 0.5 mm·min^{-1} for all tensile tests.

A typical force-extension curve recorded during the tensile test is shown in Fig. 7 and shows an initial steep slope, followed by a long yielding phase, associated with moderate stress relaxation and high ultimate strains. PDAC shows a larger yielding force (~6.14 N) and higher failure strain compared with PDFP. The stress relaxation rate is reduced when compared to PDFP according to the force-extension curves. Therefore, we can conclude that PDAC shows a better adhesion capability than PDFP in these conditions.
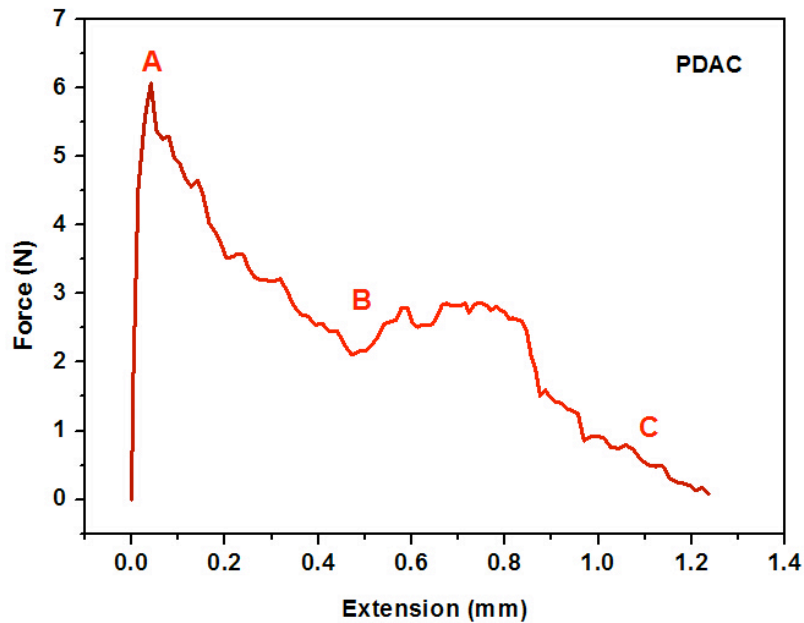
Fig. 7 - Typical force-extension curve recorded during the tensile separation of two PMMA surfaces bound by PDAC.

Three stages of deformation were characterized by SEM during the tensile test and indicated yielding (point A in Fig. 7), stress relaxation (point B in Fig. 9) and progression to failure (point C in Fig. 9). Fig. 8(A) shows scanning electron micrographs of the yielding at point A and highlights initial necking and formation of adhesive PDAC over the cross section area. This behaviour provides an initial high adhesive force between the PMMA plates. Adhesive deformation at stage B was observed using SEM and is shown in Fig. 8(B), highlighting continued necking of the adhesive fibrils that now sustain a weaker adhesive force and implies the occurrence of stress relaxation. Evidence of fibril failure within this region is observed and was found to be progress with increasing strain. As a result, the number of fibrils was considerably reduced compared to stage A, a phenomenon that underlies the gradual,

stepwise, failure of PDAC-bound interfaces. Failure of the adhesive at stage C was also characterised via SEM imaging (see Fig. 8(C)) and indicated the complete failure of adhesive fibrils. The progressive decrease of applied forces to the sample with strain is thus clearly associated with the failure of individual fibrils created at the yielding point.
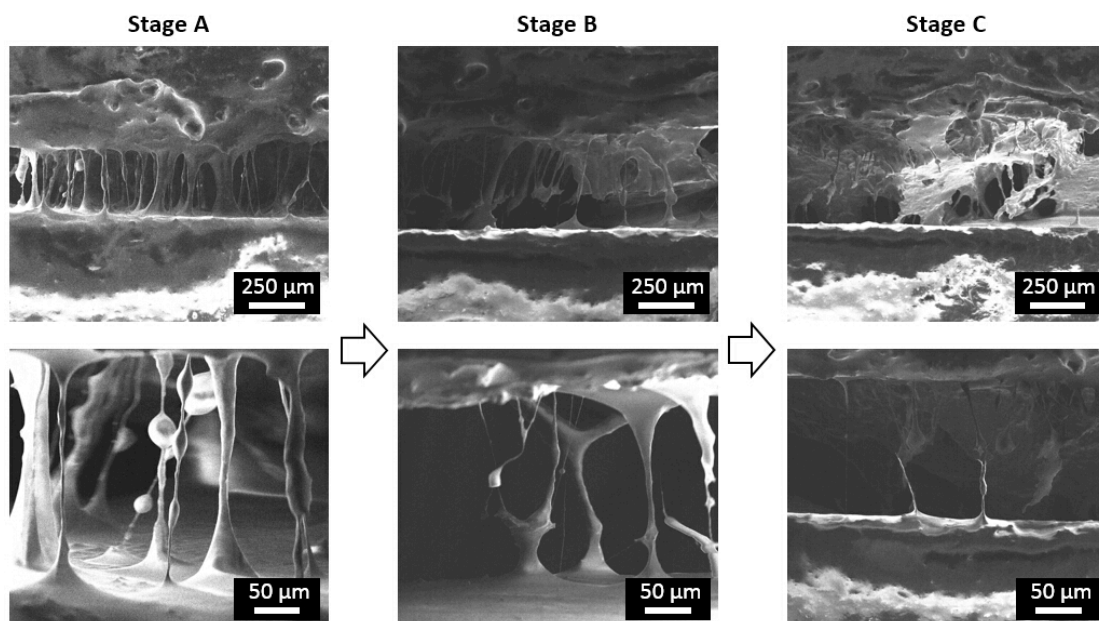
Fig. 8 - SEM micrographs at low (×200, top row) and high (×800, bottom row) magnifications showing the failure behaviour of the PDAC adhesive at stage A, B and C of Fig. 7.

In conclusion, the PDAC exhibits a higher yield force and ultimate tensile strain to failure than PDFP, with SEM imaging observing the formation of the adhesive fibrils necking at all stages until ultimate failure strain for both adhesives. Hence the failure mechanisms of PMMA plates bound with PDAC is through cohesive failure whereas PDFP fails predominantly through adhesive failure methods employing tensile testing

correlated to SEM imaging used to characterise the adhesives implies that mechanical properties of the hydrated adhesive are now dominating the failure of the bound interface. Whether this is a result of stronger interactions between PDAC and the PMMA surface or whether it arises from differences in the strength and number of fibrils formed in PDAC is not clear. Hence mechanical and adhesive testing at the nano- to micro-scale was required to elucidate the difference if failure mechanism observed between PDFP and PDAC.

3.2. Nanoscale AFM testing

Single PMMA-coated beads fixed to AFM tips were placed in contact with the adhesives and subsequently detached using the Attocube AFM in SEM as described in Section 2.2.2. All AFM tests were performed within a short period of time (<2 mins) after placing the adhesive samples into the SEM chamber to make sure that the adhesives were maintained in a hydrated condition for mechanical testing [20]. Fig. 9 presents the scanning electron micrographs of bead detachment from the adhesive shows the elongation of the adhesive into a fibril structure. A similar failure behaviour is observed in the corresponding macroscopic test and therefore indicates that the microscale testing is providing comparable fibril formation. Fig. 9 additionally shows the force-extension curves of three independent detachment tests for each adhesive. These curves highlight the occurrence of linear elastic behaviour at low extensions and plastic deformation at higher extensions. The maximum force when the interface

between the bead and the adhesive, extension at failure and the work done to failure the adhesive, found by integration of the force-extension curves, are listed in Table 2.
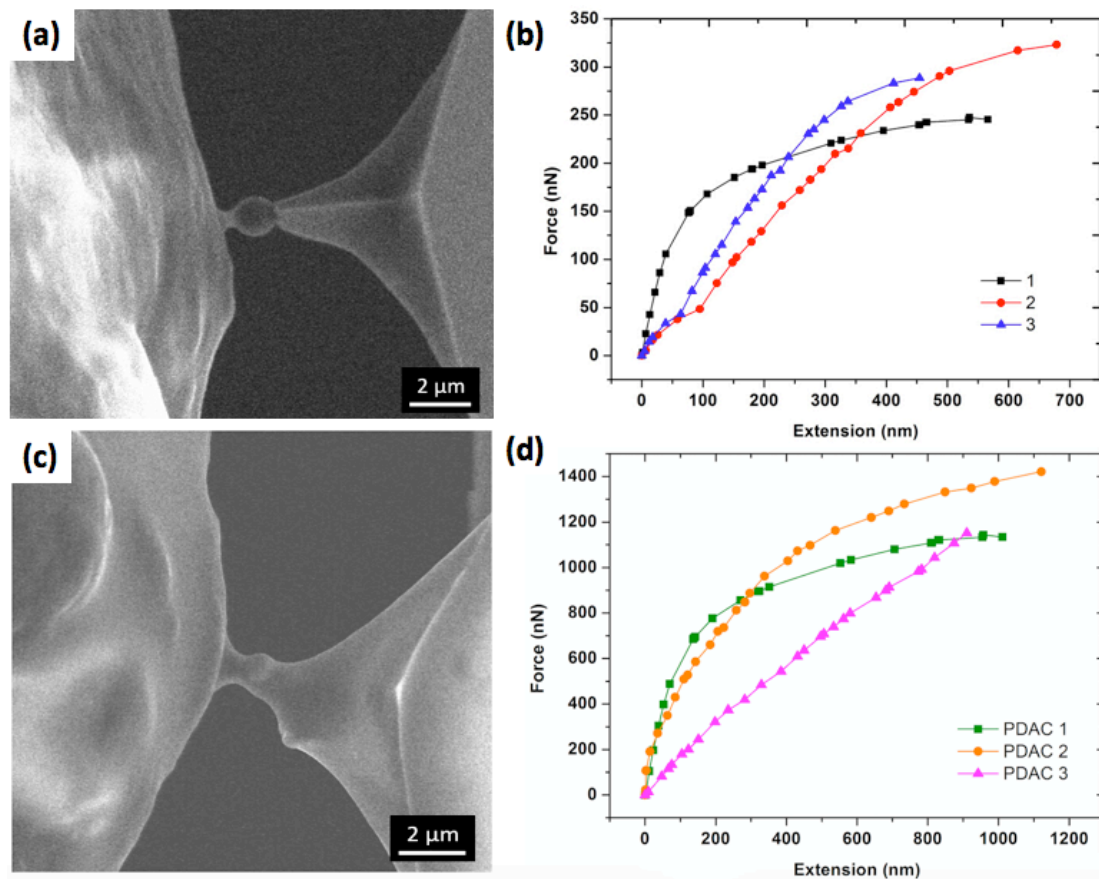
Fig. 9 - (a) Scanning electron micrograph showing the PMMA-coated bead detached from the PDFP adhesive by the Attocube AFM. (b) Force-extension curves of three successful tests on PDFP. (c) SEM micrograph showing a PMMA-coated bead detached from PDAC adhesive. (d) Corresponding force-extension curves for AFM mechanical tests on PDAC.

Table 2 - Summary of force, extension and work to failure of PMMA-bead/adhesive interfaces.

Sample	Force (nN)	Extension (nm)	Work (J)
PDFP	286 ± 39	566 ± 112	$(1.10 \pm 0.28) \times 10^{-13}$
PDAC	1234 ± 151	1016 ± 109	$(8.92 \pm 3.08) \times 10^{-12}$

The results of the macroscopic and microscopic testing provide evidence of the adhesive contribution to mechanical performance. The role of the adhesive is shown to control both the initiation of failure, presumably through the chemical interactions at the adhesive/PMMA interface, and the subsequent deformation through fibril formation until complete failure is reached. Initiation of failure is characterised by the maximum stress achieved in the linear part of the macroscopic testing that is reflected in the larger forces produced in the linear deformation region of the PDAC samples compared to the PDFP samples in the smaller scale AFM mechanical testing. The fibril formation associated with progressive failure of the adhesive in the macroscopic mechanical testing is additionally reflected in the microscale tests, where the maximum force required to fail the adhesive is highest for the PDAC sample. Interestingly, the highest force generated at the end of the linear response of the macroscopic mechanical test, labelled as point A in Fig. 3 and 7, shows an approximate six-fold increase for the PDAC sample relative to the PDFP sample, which is reflected in the maximum forces listed in Table 2 that are required to break the adhesive in the AFM mechanical tests. This multiscale mechanical approach is therefore able to provide direct relationships between the inherent material properties

of the adhesive at small length scales measured using AFM and the macroscopic mechanical behaviour.

4. Conclusions

The macroscopic mechanical behaviour of a dental adhesive fixed to PMMA surfaces representative of a denture where related to the inherent mechanical properties of the adhesive using a range of mechanical testing techniques allowing in situ observation of deformation and failure using SEM. The small scale mechanical properties of the adhesives, particularly the maximum failure strength measured using AFM, were found to control the yield and progressive failure observed macroscopically. Specifically, a PDAC adhesive exhibited considerably larger forces required for deformation and a relatively large failure force when compared to a PDFP adhesive, which correlated with larger maximum stresses and higher extensions to failure for macroscopic adhesive testing of PDAC relative to the PDFP. Design of improved adhesive formulations can therefore tune mechanical performance of the adhesive material to control overall ease of separation and removal from both denture surface and oral tissue.

5. References

[1] Xu L-C, Siedlecki CA. Effects of surface wettability and contact time on protein adhesion to biomaterial surfaces. Biomaterials. 2007;28:3273-83.

[2] An YH, Friedman RJ. Concise review of mechanisms of bacterial adhesion to biomaterial surfaces. Journal of biomedical materials research. 1998:338-48.

[3] Evans E, Ritchie K, Merkel R. Sensitive force technique to probe molecular adhesion and structural linkages at biological interfaces. Biophysical journal. 1995;68:2580.

[4] Smith BL, Schäffer TE, Viani M, Thompson JB, Frederick NA, Kindt J, et al. Molecular mechanistic origin of the toughness of natural adhesives, fibres and composites. Nature. 1999;399:761-3.

[5] Spencer P, Wang Y. Adhesive phase separation at the dentin interface under wet bonding conditions. Journal of biomedical materials research. 2002;62:447-56.

[6] Spencer P, Swafford JR. Unprotected protein at the dentin-adhesive interface. Quintessence international (Berlin, Germany: 1985). 1999;30:501-7.

[7] Spencer P, Ye Q, Park J, Topp EM, Misra A, Marangos O, et al. Adhesive/dentin interface: the weak link in the composite restoration. Annals of biomedical engineering. 2010;38:1989-2003.

[8] Grasso JE, Rendell J, Gay T. Effect of denture adhesive on the retention and stability of mixillary dentures. The Journal of prosthetic dentistry. 1994;72:399-405.

[9] Adisman IK. The use of denture adhesive as an aid to denture treatment. The Journal of prosthetic dentistry. 1989;62:711-5.

[10] Tarbet WJ, Boone M, Schmidt NF. Effect of a denture adhesive on complete denture dislodgement during mastication. The Journal of prosthetic dentistry. 1980;44:374-8.

[11] Grasso JE. Denture adhesives: changing attitudes. The Journal of the American Dental Association. 1996;127:90-6.

[12] Malacarne J, Carvalho RM, Mario F, Svizero N, Pashley DH, Tay FR, et al. Water sorption/solubility of dental adhesive resins. Dental Materials. 2006;22:973-80.

[13] Retief D. Failure at the dental adhesive—etched enamel interface. Journal of oral rehabilitation. 1974;1:265-84.

[14] Madsen F, Eberth K, Smart JD. A rheological assessment of the nature of interactions between mucoadhesive polymers and a homogenised mucus gel. Biomaterials. 1998;19:1083-92.

[15] Marshall SJ, Bayne SC, Baier R, Tomsia AP, Marshall GW. A review of adhesion science. Dental Materials. 2010;26:e11-e6.

[16] Dadarlat VM, Post CB. Adhesive–cohesive model for protein compressibility: an alternative perspective on stability. Proceedings of the National Academy of Sciences. 2003;100:14778-83.

[17] Hang F, Barber AH. Nano-mechanical properties of individual mineralized collagen fibrils from bone tissue. Journal of The Royal Society Interface. 2010;8:500-5.

[18] Hang F, Gupta HS, Barber AH. Nanointerfacial strength between non-collagenous protein and collagen fibrils in antler bone. Journal of The Royal Society Interface. 2013;11:20130993-.

[19] Hang F, Lu D, Bailey RJ, Jimenez-Palomar I, Stachewicz U, Cortes-Ballesteros B, et al. In situtensile testing of nanofibers by combining atomic force microscopy and scanning electron microscopy. Nanotechnology. 2011;22:365708.

[20] Jimenez-Palomar I, Shipov A, Shahar R, Barber AH. Influence of SEM vacuum on bone micromechanics using in situ AFM. Journal of the Mechanical Behavior of Biomedical Materials. 2012;5:149-55.

[21] Wang C, Frogley MD, Cinque G, Liu L-Q, Barber AH. Deformation and failure mechanisms in graphene oxide paper using in situ nanomechanical tensile testing. Carbon. 2013;63:471-7.

[22] Guo X, Deng F, Li L, Prud'homme RK. Synthesis of biocompatible polymeric hydrogels with tunable adhesion to both hydrophobic and hydrophilic surfaces. Biomacromolecules. 2008;9:1637-42.

[23] Tan KY, Gautrot JE, Huck WT. Formation of Pickering Emulsions Using Ion-Specific Responsive Colloids†. Langmuir. 2010;27:1251-9.

[24] Tan KY, Lin H, Ramstedt M, Watt FM, Huck WT, Gautrot JE. Decoupling geometrical and chemical cues directing epidermal stem cell fate on polymer brush-based cell micro-patterns. Integrative Biology. 2013;5:899-910.

[25] Sader JE, Larson I, Mulvaney P, White LR. Method for the calibration of atomic force microscope cantilevers. Review of Scientific Instruments. 1995;66:3789-98.

[26] Kramer EJ, Berger LL. Fundamental processes of craze growth and fracture. Crazing in Polymers Vol 2: Springer; 1990. p. 1-68.